Numerical Simulation of the Power Density Distribution Generated in a Multimode Cavity by Using the Method of Lines Technique to Solve Directly for the Electric Field

Huawei Zhao, Ian Turner, and Fa-Wang Liu

Abstract—**In this paper, a new numerical method is presented in order illustrate how the Method of Lines technique can be used to obtain the power density distribution in a dielectric material by solving directly for the electric field in three-dimensional space. A detailed analysis of the treatment of the boundary conditions at the interfaces that exist between air and the material, as well as at absorbing boundary and input planes, are also given in this paper. The method is tested and verified on some simple waveguide examples for which analytic solutions are available. The technique is subsequently applied to the more complicated cavity problem and the solutions for the power density distribution are compared directly with those obtained in previous research using the finite-difference time-domain (FDTD) method. The results of all tests conducted in this research indicate that the Method of Lines technique is a robust numerical tool which can be used to readily handle the hyperbolic nature of the Maxwell equations. Finally, in order to demonstrate the versatility of the developed model, the power density distribution generated inside a dielectric material loaded in a cavity that has multiple input waveguides is presented. The chosen examples exhibit the complicated electromagnetic phenomena which arise inside the cavity and provides some idea of the effect of multiple waveguide input on the power density distribution.**

I. Introduction

MICROWAVE heating has been used widely in a number of industrial heating and drying processes [1]–[4]. Two of the major problems associated with microwave heating are the phenomena of arc-over and the spatial nonuniformity of the microwave field strength, which causes localized hot or cold spots to arise at sometimes random locations within the applicators [5], [6]. In order to gain insight into the phenomena that occur inside the microwave cavity, a detailed knowledge of the electric and magnetic fields, together with a prediction of the power distribution in the dielectric material is necessary. In previous research the finite-difference time-domain (FDTD) method [3], [4], [7] has been shown to be an applicable numerical solution technique for solving the Maxwell's equations in the microwave heating applicator. Since this technique has been validated earlier by the authors, the FDTD solutions will be used to benchmark the performance of the new numerical scheme proposed in this paper when an analytic solution is not available.

The Method of Lines (MoL) is a well-known technique for solving parabolic type partial differential equations [8]. Essentially, the MoL technique proceeds by leaving the derivatives along one chosen axis untouched (usually in time), while all other partial derivatives (usually in space) are discretised using well-known strategies that include the finite difference, finite element, or finite volume techniques. The system is thereby reduced from its partial differential form to a system of ordinary differential equations that can be solved numerically by standard procedures such as Runge-Kutta or Predictor-Corrector schemes, or by more sophisticated software packages [9]. Recently, the MoL [10], [11] has been used to solve Maxwell's equations directly for the magnetic field (MAXMOL-H). It should be noted, however, that in order to deduce the power density distribution in the cavity, the magnetic field has to be curled to provide the electric field and this can lead to a substantial computational overhead, since numerical derivatives must be constructed. Nevertheless, the scheme highlighted that the MoL has been successfully employed to solve the hyperbolic Maxwell equations.

In this paper, a new numerical treatment is presented for solving Maxwell's equations whereby the MoL technique is employed to resolve the electric field directly (MAXMOL-E). A different strategy to that proposed in [10] and [11] is utilized, and numerical models that solve Maxwell's equations for either the magnetic field system or the electric field system have been implemented to gauge their performances. A detailed synopsis of MAXMOL-E will be given here. The results of numerous numerical experiments has indicated that both schemes provide accurate results, however, using MAXMOL-E appears to be more convenient and computationally efficient in comparison with MAXMOL-H, since the power density distribution can be obtained directly from the electric field distribution. In fact, when the convergence criterion of these numerical schemes is based on the analysis of the power distribution, MAXMOL-E is always more computationally efficient in comparison with MAXMOL-H. There are also other convergence criteria, however, that may be used to terminate the iteration of these numerical schemes. For example, it is possible to consider the maximum and minimum

Manuscript received September 22, 1995; revised August 26, 1996.

The authors are with the School of Mathematics, Queensland University of Technology, Brisbane, Queensland 4001, Australia.

Publisher Item Identifier S 0018-9480(96)08485-2.

changes in the relevant fields through a given period as a convergence indicator. Nevertheless, because the primary concern of microwave heating problems concerns achieving a sinusoidal steady state power distribution, it has been decided to use a convergence indicator based on that distribution for all the tests undertaken in this research.

The main focus of this research concerns the application of the MoL for solving the three-dimensional (3-D) time-dependent Maxwell's Equations for the electric field. The solutions obtained from the model are verified against some analytical solutions for a rectangular waveguide loaded with a dielectric material. The model is subsequently applied to the more complicated cavity problem and the solutions for the power density distribution are compared directly with those obtained in previous research using the FDTD method. Finally, in order to demonstrate the versatility of the developed model and to test further the performance of the method under extremely harsh numerical conditions, the power density distribution generated inside a dielectric material loaded in a multimode cavity that is fed by multiple input waveguides each operating at the same frequency of 2450 MHz is studied. The chosen examples exhibit the complicated electromagnetic phenomena that arise inside the cavity and provides some idea of the effect of multiple waveguide input on the power density distribution

The paper is organized as follows: In Section II, the basic equations of the method of lines MAXMOL-E are described. In Section III, the boundary conditions and their numerical treatment are presented. In Section IV, the dissipated power is calculated. The results are discussed in Section V, and finally, the conclusion is given.

II. Basic Equations

Starting from Maxwell's Equations, the derivation is similar to that found in [3] and [4], however here we eliminate the magnetic field $\boldsymbol{H}$ and obtain a hyperbolic system of partial differential equations for the electric field $\boldsymbol{E}$ given in nondimensional form as follows:

$$\varepsilon' \frac{\partial^2 \hat{\boldsymbol{E}}}{\partial \hat{t}^2} = -\nabla \times \nabla \times \hat{\boldsymbol{E}} - s\hat{\boldsymbol{E}} - \sigma^* \frac{\partial \hat{\boldsymbol{E}}}{\partial \hat{t}} \tag{1}$$

and in the cartesian coordinate system (x, y, z) as

$$\begin{aligned}
\varepsilon' \frac{\partial^2 \hat{E}_x}{\partial \hat{t}^2} &= \left(\frac{\partial^2 \hat{E}_x}{\partial y^2} + \frac{\partial^2 \hat{E}_x}{\partial z^2} - \frac{\partial^2 \hat{E}_y}{\partial x \partial y} - \frac{\partial^2 \hat{E}_z}{\partial x \partial z} \right) - s\hat{E}_x \\
&\quad - \sigma^* \frac{\partial \hat{E}_x}{\partial \hat{t}} \\
\varepsilon' \frac{\partial^2 \hat{E}_y}{\partial \hat{t}^2} &= \left(\frac{\partial^2 \hat{E}_y}{\partial z^2} + \frac{\partial^2 \hat{E}_y}{\partial x^2} - \frac{\partial^2 \hat{E}_z}{\partial y \partial z} - \frac{\partial^2 \hat{E}_x}{\partial y \partial x} \right) - s\hat{E}_y \\
&\quad - \sigma^* \frac{\partial \hat{E}_y}{\partial \hat{t}} \\
\varepsilon' \frac{\partial^2 \hat{E}_z}{\partial \hat{t}^2} &= \left(\frac{\partial^2 \hat{E}_z}{\partial x^2} + \frac{\partial^2 \hat{E}_z}{\partial y^2} - \frac{\partial^2 \hat{E}_x}{\partial z \partial x} - \frac{\partial^2 \hat{E}_y}{\partial z \partial y} \right) - s\hat{E}_z \\
&\quad - \sigma^* \frac{\partial \hat{E}_z}{\partial \hat{t}}
\end{aligned} \tag{2}$$

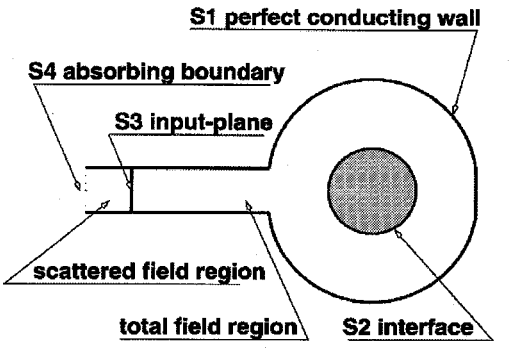

Fig. 1. Boundary conditions.

where

$$\begin{aligned}
s &= T^{*2}\left(\frac{\partial^2 \varepsilon'}{\partial \hat{t}^2} + \omega \frac{\partial \varepsilon''}{\partial t} \right) \\
\sigma^* &= T^*\left(2\frac{\partial \varepsilon'}{\partial t} + \omega \varepsilon'' \right) \\
\hat{\boldsymbol{E}} &= \boldsymbol{E}/E_0 \\
\hat{t} &= t/T^* \\
\boldsymbol{r} &= (x, y, z) = (X/L^*, Y/L^*, Z/L^*) \\
L^* &= C_0 T^*.
\end{aligned}$$

s is the nonlinear effective factor of the dielctric material, σ^* is an effective conductivity of the dielectric material, ε' is the real relative permittivity, ε'' is the effective loss factor, ω the angular frequency, E_0 is the electric field intensity scale (V/m), T^* is the time scale (s), L^* is the length scale (m), and C_0 is the speed of light. We assume that the material properties are piece-wise continuous in space having discontinuities only at air–material interfaces. These properties may be functions of temperature. It is also assumed that the material is not magnetic so that $(\mu = \mu_0)$.

Equation (1) can be written as the following pair of first-order equations in time:

$$\frac{\partial \hat{\boldsymbol{E}}}{\partial \hat{t}} = \boldsymbol{\Phi} \tag{3}$$

$$\frac{\partial \boldsymbol{\Phi}}{\partial \hat{t}} = \frac{1}{\varepsilon'}(-\nabla \times \nabla \times \hat{\boldsymbol{E}} - s\hat{\boldsymbol{E}} - \sigma^* \boldsymbol{\Phi}). \tag{4}$$

By discretising the spatial derivatives in (2) on a 3-D mesh using second-order central difference approximations, for example

$$\frac{\partial^2 \hat{E}_x}{\partial y^2} = \frac{1}{\delta y^2}(\hat{E}_{x(i,j-1,k)} - 2\hat{E}_{x(i,j,k)} + \hat{E}_{x(i,j+1,k)}) \tag{5}$$

$$\begin{aligned}
\frac{\partial^2 \hat{E}_y}{\partial x \partial y} &= \frac{1}{4\delta x \delta y}(\hat{E}_{y(i-1,j-1,k)} + \hat{E}_{y(i+1,j+1,k)} \\
&\quad - \hat{E}_{y(i-1,j+1,k)} - \hat{E}_{y(i+1,j-1,k)})
\end{aligned} \tag{6}$$

a system of first-order ordinary differential equations is obtained

$$\frac{d\hat{\boldsymbol{E}}_{i,j,k}}{d\hat{t}} = \boldsymbol{\Phi}_{i,j,k} \tag{7}$$

$$\frac{d\boldsymbol{\Phi}_{i,j,k}}{d\hat{t}} = \boldsymbol{\Psi}_{i,j,k}(\boldsymbol{\Phi}, \hat{\boldsymbol{E}}, \hat{t}) \tag{8}$$

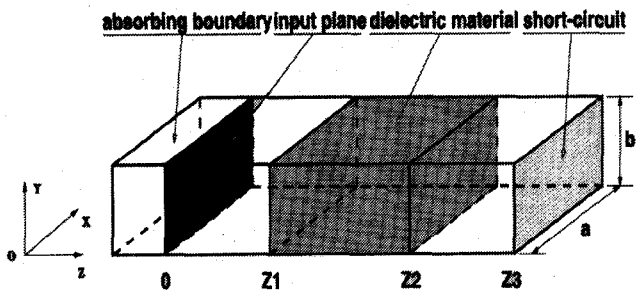

Fig. 2. Lossy slab in a rectangular waveguide.

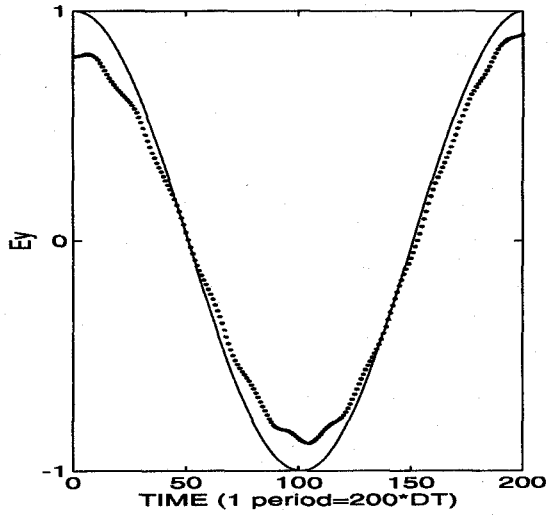

Fig. 3. Approximation of absorbing boundary condition for Test 1 (a) The Taylor Series approximation $(\cdots)$ against analytical solution (___) (b) The Method of characteristics approximation $(\cdots)$ against analytical solution (___).

where $\boldsymbol{\Phi}_{i,j,k}$ and $\hat{\boldsymbol{E}}_{i,j,k}$ represent the values of $\boldsymbol{\Phi}$ and $\hat{\boldsymbol{E}}$ at the point (i,j,k), and $\boldsymbol{\Psi}_{i,j,k}$ represents the finite difference expression of the right-hand side of (4) at the point (i,j,k), where δx and δy denote the space increments.

The study of stability for the MoL technique, as applied to Maxwell's equations, can be analyzed by the von Neumann

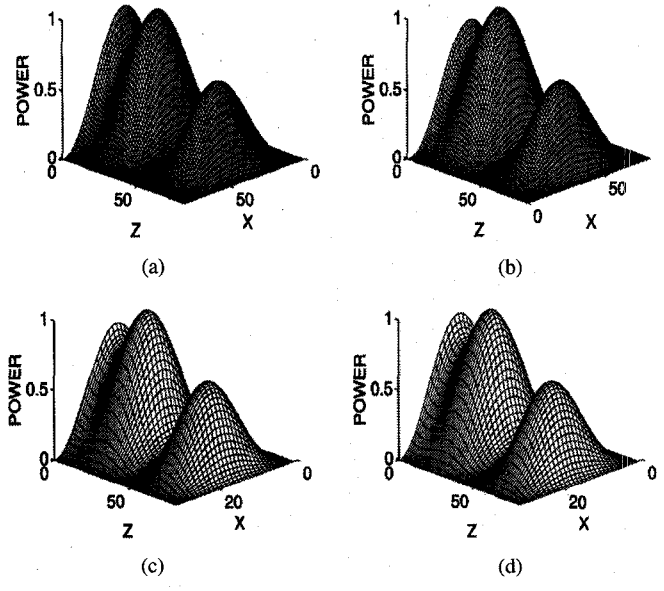

Fig. 4. Comparison of the power density distribution for the Analytical, FD–TD, MAXMOL-H, and MAXMOL-E methods for Test 2.

method, the results in [11] are given as

$$\delta\hat{t} \ll \min\left(2\frac{\varepsilon'}{\sigma^*}\right) \tag{9}$$

$$\max\left[\frac{\delta\hat{t}}{(\varepsilon')^{1/2}}\right] < \delta L < \min\left[\frac{(8\varepsilon')^{1/2}}{\sigma^*}\right] \tag{10}$$

where

$$\left(\frac{1}{\delta L}\right)^2 = \left(\frac{1}{\delta x}\right)^2 + \left(\frac{1}{\delta y}\right)^2 + \left(\frac{1}{\delta z}\right)^2.$$

III. Boundary Conditions and Numerical Treatment

To obtain a well posed set of the Maxwell's equations that can be solved numerically, boundary conditions have to defined. From Fig. 1, the boundary of the problem under consideration can be thought to consists of four different surfaces $\boldsymbol{S}_1, \boldsymbol{S}_2, \boldsymbol{S}_3$ and $\boldsymbol{S}_4$, which correspond to a perfectly conducting surface, the interface between air and a dielectric material, the power input plane, and the absorbing boundary condition, respectively.

$\boldsymbol{S}_1$ at a perfect electrically conducting surface requires the following two constraints [12].

1) The tangential components of the $\boldsymbol{E}$ field are zero.
2) The derivatives of the normal component of the $\boldsymbol{E}$ field in the normal direction are zero.

$\boldsymbol{S}_2$ at an interface between air and the dielectric material requires the following two boundary conditions to be satisfied [12]:

$$\boldsymbol{n} \times (\boldsymbol{E}_2 - \boldsymbol{E}_1) = \boldsymbol{0} \tag{11}$$

$$\boldsymbol{n} \cdot (\varepsilon_2 \boldsymbol{E}_2 - \varepsilon_1 \boldsymbol{E}_1) = 0. \tag{12}$$

From (11) and (12), the tangential components of the $\boldsymbol{E}$ field are continuous across a dielectric interface, the normal component of the $\boldsymbol{E}$ field is discontinuous across a dielectric interface, and its first- and second-order derivatives may also be discontinuous across that interface. Consequently, it is not possible to use approximations like (5) and (6) at the interface between air and the dielectric material. A simple and

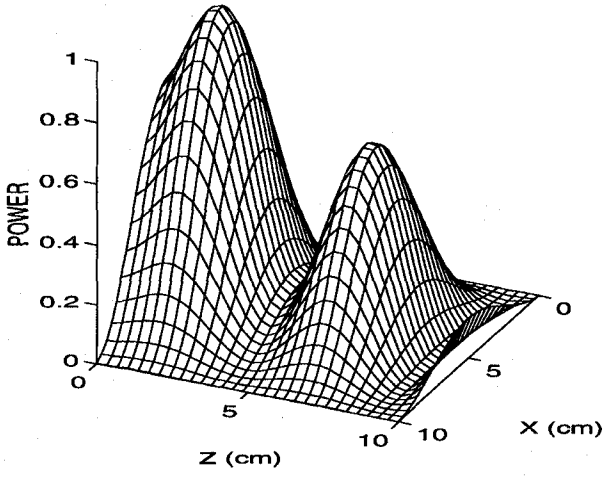

(a)

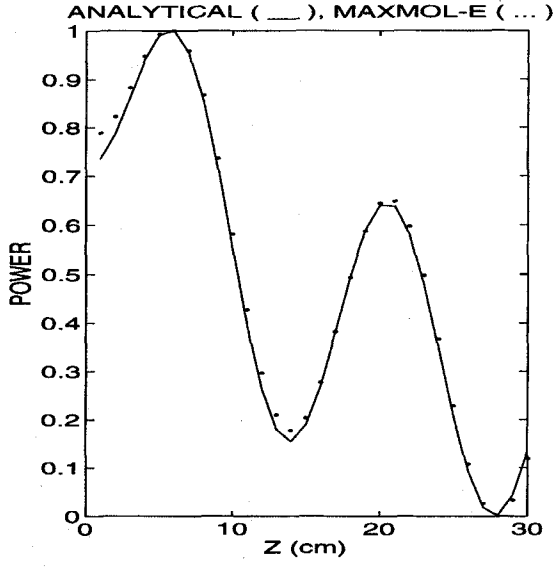

(b)

Fig. 5. Comparison of the power density distribution of the analytical and MAXMOL-E methods for Test 3.

accurate method, which automatically takes full account of the discontinuities in the normal electric field components across any arbitrary distribution of internal dielectric interfaces, is presented by Stern [13] for the determination of the polarized solutions of the Helmholtz wave equation. Using this technique, Fu and Metaxas [10], [11] obtained an approximation for $\nabla^2 \boldsymbol{H}$ across a dielectric interface. Here, using the same technique, we obtain for the components $\boldsymbol{E}$ normal across an interface, in the y direction

$$\frac{\partial^2 \hat{E}_y}{\partial y^2} = \frac{1}{\delta y^2}(D_1 \hat{E}_{y(i,j-1,k)} - (D_2 + D_3)\hat{E}_{y(i,j,k)} + D_4 \hat{E}_{y(i,j+1,k)}) \tag{13}$$

where

$$D_1 = 2\varepsilon'_{(i,j-1,k)}/(\varepsilon'_{(i,j,k)} + \varepsilon'_{(i,j-1,k)})$$
$$D_2 = 2\varepsilon'_{(i,j,k)}/(\varepsilon'_{(i,j,k)} + \varepsilon'_{(i,j-1,k)})$$
$$D_3 = 2\varepsilon'_{(i,j,k)}/(\varepsilon'_{(i,j,k)} + \varepsilon'_{(i,j+1,k)})$$
$$D_4 = 2\varepsilon'_{(i,j+1,k)}/(\varepsilon'_{(i,j,k)} + \varepsilon'_{(i,j+1,k)})$$

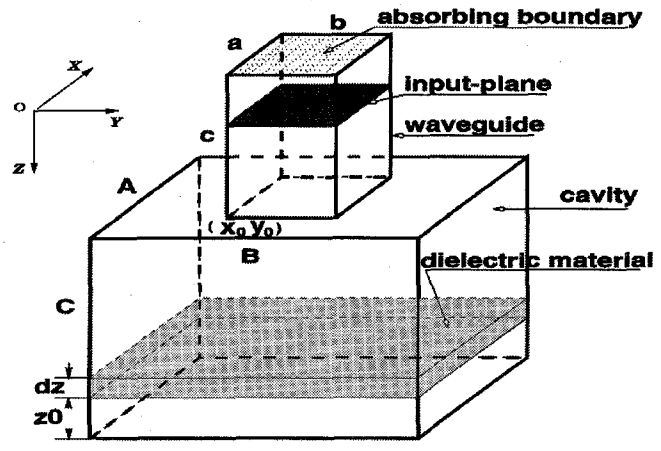

Fig. 6. Rectangular cavity excited by a single waveguide.

for the tangential components of $\boldsymbol{E}$ across an interface in the x direction

$$\frac{\partial^2 \hat{E}_y}{\partial x^2} = \frac{1}{\delta x^2}(T_1 \hat{E}_{y(i-1,j,k)} - (T_1 + T_2)\hat{E}_{y(i,j,k)} + T_2 \hat{E}_{y(i+1,j,k)}) \tag{14}$$

where

$$T_1 = 2\beta_{(i,j,k)}/(\beta_{(i,j,k)} + \beta_{(i-1,j,k)})$$
$$T_2 = 2\beta_{(i,j,k)}/(\beta_{(i,j,k)} + \beta_{(i+1,j,k)})$$

and [14]

$$\beta \propto \sqrt{\varepsilon'\left(1 + \sqrt{1 + \left(\frac{\varepsilon''}{\varepsilon'}\right)^2}\right)}.$$

Further details can be found in the Appendix.

$\boldsymbol{S}_3$ at an input plane requires that the input plane divides the system into two separate regions, the total field region and the scattered field region [7], [3]. On the input plane the incident wave must be defined, and the input wave only propagates in the positive direction. This implies that we have to make a correction to the derivatives with respect to the wave propagating direction, for example

$$\frac{\partial^2 \hat{E}_{y(i,j,k_{in})}}{\partial z^2} = \frac{1}{\delta z^2}[\hat{E}_{y(i,j,k_{in}-1)} - 2\hat{E}_{y(i,j,k_{in})} + (\hat{E}_{y(i,j,k_{in}+1)} - \hat{E}_{y-in(i,j,k_{in}+1)})] \tag{15}$$

$$\frac{\partial^2 \hat{E}_{y(i,j,k_{in}+1)}}{\partial z^2} = \frac{1}{\delta z^2}[(\hat{E}_{y(i,j,k_{in})} + \hat{E}_{y-in(i,j,k_{in})}) - 2\hat{E}_{y(i,j,k_{in}+1)} + \hat{E}_{y(i,j,k_{in}+2)}]. \tag{16}$$

For a TE_{10} mode the incident wave can defined as follows:

$$\hat{E}_{y\text{-in}} = \hat{E}_0 \sin\frac{\pi x}{a}\cos\omega t \tag{17}$$

where E_0 is the amplitude of the input wave, a is the width of the waveguide, and ω is the angular frequency of the incident wave.

$\boldsymbol{S}_4$ at an absorbing plane requires that in the waveguide region, behind the waveguide input plane, there is only a reflected wave. The fields in the terminal plane cannot be determined by the MoL scheme. We have to set an absorbing

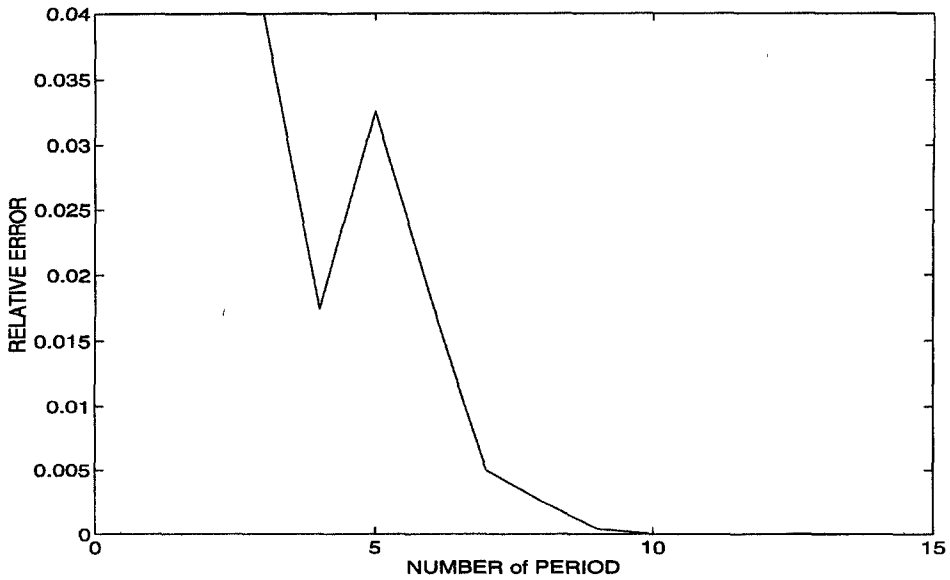

Fig. 7. The convergence of iteration for MAXMOL-E Test 4.

boundary condition to enable the mesh to be truncated by means of an artificial boundary which simulates the unbounded surroundings. The absorbing boundary is given as [7], [15]

$$\left(\frac{\partial}{\partial z} - \frac{1}{C_0}\frac{\partial}{\partial t}\right) E_y|_{z=z_0} = 0. \tag{18}$$

The following two possibilities for discretizing this boundary condition and utilizing it within the system are considered: 1) By constructing a Taylor series, which is a second-order accurate approximation

$$\hat{E}^{n+1}_{y(i,j,-1)} = \hat{E}^{n}_{y(i,j,0)} - \frac{L^*\delta z}{c_0 T^*}\left[\frac{3}{8}\Phi^n_{y(i,j,0)} + \frac{3}{4}\Phi^n_{y(i,j,1)} - \frac{1}{8}\Phi^n_{y(i,j,2)}\right]. \tag{19}$$

2) By using the method of characteristics: from (18), the line is given as

$$\delta z = -C^*\delta\hat{t} \tag{20}$$

where

$$C^* = \frac{C_0 T^*}{L^*} \tag{21}$$

by setting

$$\frac{C^*\delta\hat{t}}{\delta z} = \lambda \tag{22}$$

and using liner interprolation, we obtain

$$\frac{\hat{E}^n_{y(i,j,-1)} - \hat{E}^{n+1}_{y(i,j,-1)}}{\hat{E}^n_{y(i,j,-1)} - \hat{E}^n_{y(i,j,0)}} = \lambda \tag{23}$$

so that (18) gives

$$\hat{E}^{n+1}_{y(i,j,-1)} = \hat{E}^n_{y(i,j,-1)} - \lambda[\hat{E}^n_{y(i,j,-1)} - \hat{E}^n_{y(i,j,0)}]. \tag{24}$$

IV. Calculation of the Dissipated Power

In the MAXMOL-E scheme, once a steady-state solution is achieved, the average dissipated power has to be taken into account by taking the average over a period of time, i.e.,

$$P^{\tau}_{\sigma\mathrm{av}(i,j,k)} = \frac{1}{N}\sigma_{e(i,j,k)}\sum_{n=1}^{N} \boldsymbol{E}^n_{(i,j,k)} \cdot \boldsymbol{E}^n_{(i,j,k)} \tag{25}$$

where

$$\sigma_{e(i,j,k)} = \omega\varepsilon_0\varepsilon''_{(i,j,k)}.$$

N is the number of time steps in each period of time and τ is the number of the period.

To control the convergence of the iterations, the following relative least square error test is used [3]

$$Rerror = \frac{\sqrt{\sum_{(i,j,k)\in \boldsymbol{M}} (P^{\tau}_{\sigma\mathrm{av}(i,j,k)} - P^{\tau-1}_{\sigma\mathrm{av}(i,j,k)})^2}}{\sum_{(i,j,k)\in \boldsymbol{M}} P^{\tau}_{\sigma\mathrm{av}(i,j,k)}} \leq \mathrm{tol} \tag{26}$$

where $\boldsymbol{M}$ is a set of points that are in the dielectric material and tol is a given tolerant parameter and $P^{\tau}_{\sigma\mathrm{av}(i,j,k)}$ and $P^{\tau-1}_{\sigma\mathrm{av}(i,j,k)}$ denote the power density at a point (i, j, k) in the two different periods, respectively.

V. Results and Discussion

The results presented in this section were computed using a Dec ALPHA workstation and the power density distributions are displayed in normalized form. In order to assess the performance and validate the MAXMOL-E scheme, five tests have been performed for two different configurations. The first configuration tested concerns the microwave irradiation of a

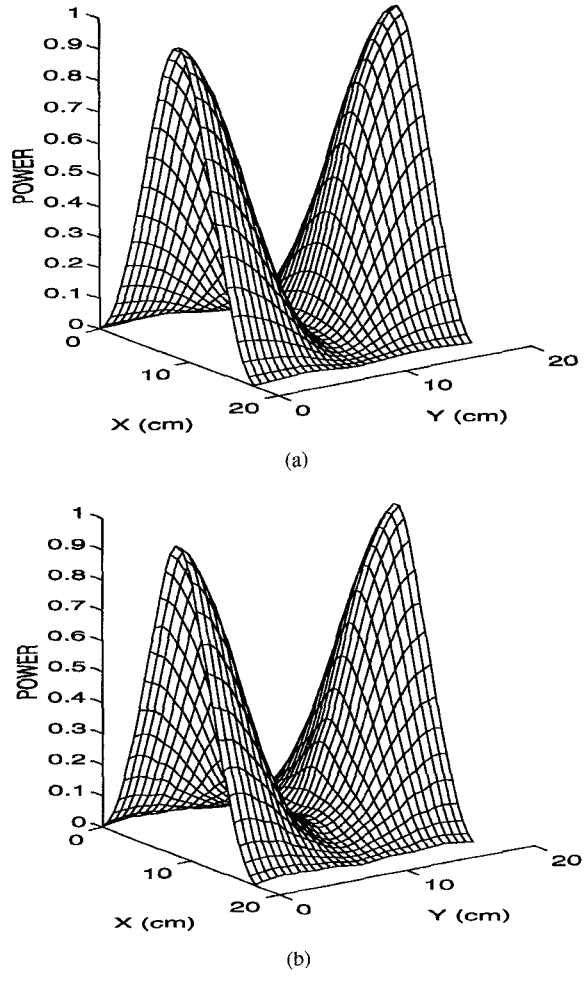

Fig. 8. Comparison of the power density distribution of FDTD and MAXMOL-E methods for the cavity in Test 4; the dielctric material is located at the bottom of the cavity with $z0 = 0.0$ cm.

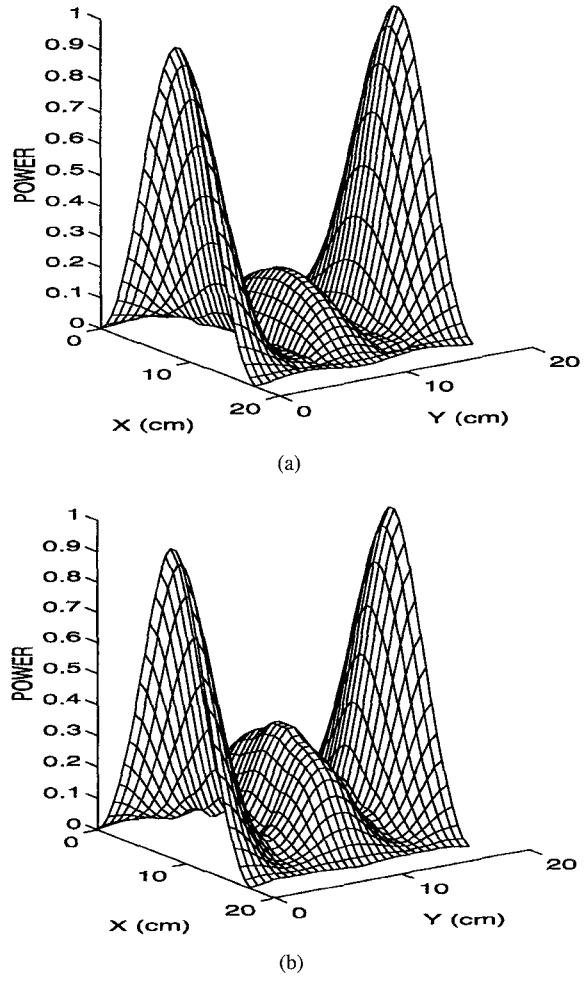

Fig. 9. Comparison of the power density distribution of FDTD and MAXMOL-E methods for the cavity in Test 4, the dielectric material is located at $z0 = 4.587$ cm from the bottom of the cavity.

dielectric material loaded at different locations within a rectangular waveguide. For this case standard analytic solutions are available and the results of MAXMOL-E can be easily verified. Further, in order to demonstrate the accuracy of the method of characteristics approximation for the absorbing boundary condition a simple example is analyzed. Once the results of MAXMOL-E were in good agreement with the analytical solutions it was decided for the second configuration to test the more complicated case of a dielectric material loaded within a multimode cavity. Since in this case it was not possible to derive analytical solutions, the results of MAXMOL-E were compared with the results previously published for the same case using the FD–TD method [3]. The effects on the power density distribution of moving the material to different locations within the cavity or using multiple input waveguides are also analyzed.

For all cases studied the dielectric material properties are assumed piece-wise constant. The input plane is excited at the microwave frequency of 2.45 GHz, and the TE_{10} mode is the dominant mode inside the waveguide. Table I gives the mesh dimensions and the CPU time taken for the first three test cases. The time step size was chosen as $\delta t = 2.04$ ps so that the stability criteria given in (9) and (10) are satisfied. Equation (26) is used for determining the converge criterion of both MAXMOL schemes, where a value of tol = 0.000 05 implies that the computation will terminate somewhere between 10 and 15 periods of processing.

The first configuration tested is a rectangular waveguide filled with a lossy material and terminated by a short circuit, shown in Fig. 2. The waveguide dimension is $a = 10$ cm, $b = 5$ cm. The parameters z_1, z_2, and z_3 are specified for each test case.

1) Test 1—Accuracy of the Absorbing Boundary Condition: This test problem is a special case of that exhibited in Fig. 2, where here the accuracy of the absorbing boundary condition is analyzed. In this case there is no material loaded in the waveguide and at one end of the waveguide the input plane is located, while at the other end, at $z_3 = 2\lambda_g = 30.97$ cm there is only an absorbing boundary condition instead short-circuit. Since this is such a simple model, with the microwaves launched from the input plane and vanishing at the absorbing boundary, there is no reflected wave existing inside the waveguide. As was stated above, the absorbing boundary condition can be approximated by two different methods, and

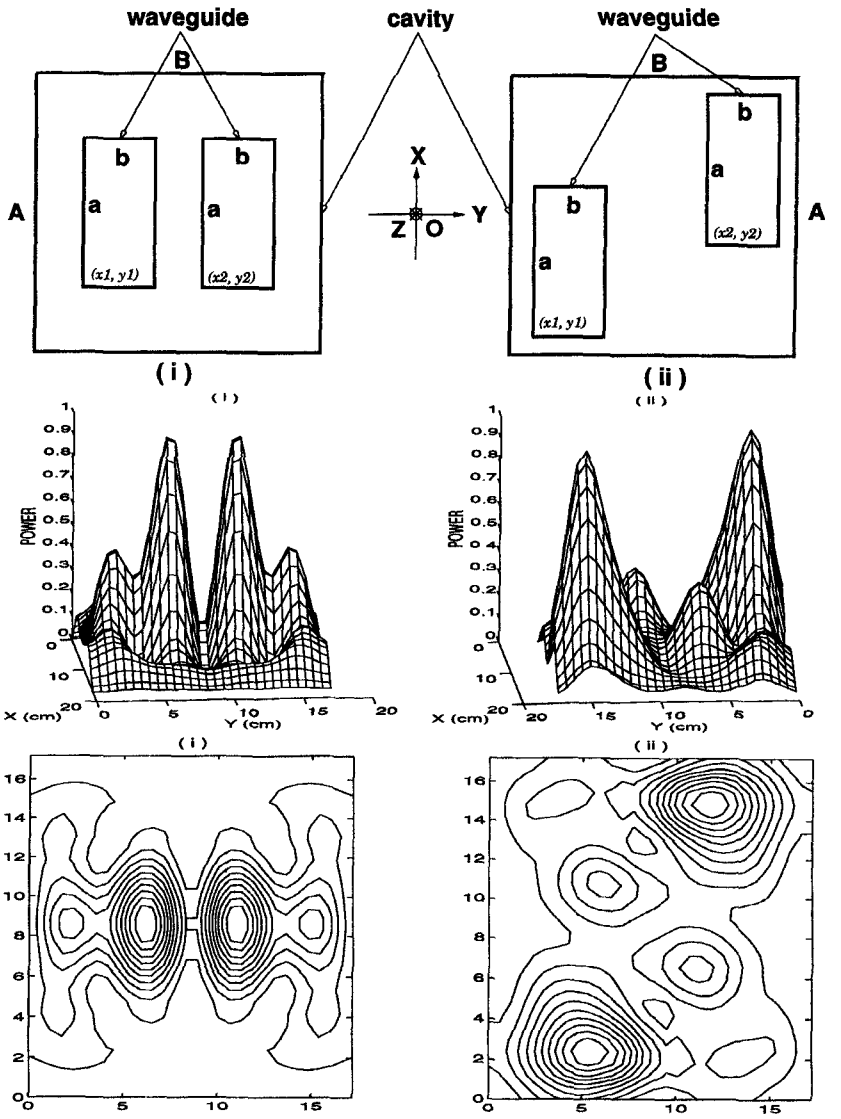

Fig. 10. Rectangular cavity excited by two waveguides.

the results of these approximations are given in Fig. 3. In the past, the absorbing boundary condition has been employed in the FDTD method [7], [3], [4], where it was approximated by finite differences and linear interpolation. The results appear that the method of characteristics (MoC) almost identical with the analytical solution and are far better than those obtained for the Taylor series approximation. Furthermore, the use of the MoC can offer a reduction in the overall processing time (see Table I), as opposed to the Taylor method. As a consequence of these findings the MoC is implemented in all of the following tests.

2) Test 2—Lossy Material Loaded Adjacent to the Short Circuit Boundary: This case is equivalent to the problem tested by Jia and Jolly [1992] where the dielectric property of the lossy material was assumed constant at $\varepsilon_r = 2.0 - 0.5j$ and $z_1 = 10$ cm and $z_2 = z_3 = 20$ cm. The results given by the analytical solution, the FDTD scheme, MAXMOL-H (the model implemented here for MAXMOL-H uses the same techniques for discretization and boundary conditions discussed in this paper and is therefore a slight variation of the model presented in [10] and [11] MAXMOL-E are shown in Fig. 4. Through the comparison of those four solutions, it is possible to observe that they are all in good agreement, with the numerical models predicting the same shape and magnitude of the analytical solution. From Table I, however, it is clear that the MAXMOL-E is approximately twice as fast as MAXMOL-H. The increased execution time of the MAXMOL-H scheme can be explained by the following facts: for the waveguide problem, both the (H_x and H_z) distributions must be computed and then the resulting magnetic field has to be converted to the electric field in order to calculate the power density distribution. For the MAXMOL-E scheme only, however, (E_y) is computed and the power distribution can be deduced directly.

3) Test 3—Lossy Material Loaded at the Center of the Waveguide: For this case the lossy slab is located at the centre of the waveguide applicator with $z_1 = 10$ cm, $z_2 = 20$ cm, and $z_3 = 30$ cm. The dielectric property of the material is again assumed constant at $\varepsilon_r = 2.0 - 0.5j$. The results given by the analytical solution and MAXMOL-E are shown in Fig. 5. In

this case, the solution of the power density distribution given by the MAXMOL-E scheme exhibits a remarkable match with the analytical solution. Furthermore, it can be seen from Table I that MAXMOL-E is approximately twice as fast as MAXMOL-H.

At this point the MAXMOL-E scheme has been tested against some standard analytical solutions and has shown good agreement. Having validated satisfactorily the MAXMOL-E numerical method, it is now possible to continue to test this scheme with good confidence for the second configuration which concerns the more complicated multimode cavity case. This example represents a good challenge for the numerical model and in order to verify the accuracy of MAXMOL-E the obtained predictions will be validated against those previously computed by the FDTD scheme.

4) Test 4—Lossy Material Loaded Within a Multimode Cavity: This test problem represents the medium-sized cavity shown in Fig. 6, where $A = 17.2$ (cm), $B = 17.2$ (cm), $C = 14.907$ (cm), $a = 9.173$ (cm), $b = 4.586$ (cm), and $c = 11.466$ (cm). The space increments are $30\delta x \times 30\delta y \times 26\delta z$ in the cavity and $16\delta x \times 8\delta y \times 20\delta z$ in the waveguide. The input plane is located at a position $10\delta z$ from the absorbing boundary, and the waveguide is located at $x_0 = 7\delta x$ and $y_0 = 11\delta y$. The dielectric material is loaded in the X-Y plane with a thickness of $dz = 3\delta z$, at two different locations $z_0 = 0.0$ cm and $z_0 = 4.587$ (cm). The relative permittivity is $\varepsilon_r = 2.0 - 0.5j$.

For this case an analysis of the convergence of the MAXMOL-E scheme using (26) is shown in Fig. 7. It can be seen that after ten periods have transpired, the solution of the average power density distribution has reached the sinusoidal steaded state solution.

From Figs. 8 and 9, it is clear that the simulation results obtained by the MAXMOL-E scheme resemble the results obtained from the FDTD scheme, with the shape of the solution being similar. Furthermore, it is noticable that the biggest difference occurs in the center of the material in Fig. 9, however the overall trends of both solutions and qualitatively equivalent.

Finally, in order to demonstrate the versatility of the developed MAXMOL-E model, the power density distribution generated inside a dielectric material loaded in a multimode cavity, which is fed by multiple input waveguides, is studied. The chosen examples exhibit the complicated electromagnetic phenomena that arise inside the cavity and provides some insight of the effect of multiple waveguide input on the power density distribution. With the knowledge obtained from such studies, it may be possible to numerically optimize the cavity design in order to achieve a uniform heating phenomenon to arise within the material loaded within the cavity. This idea forms the basis of future research.

5) Test 5—The Infleuence of Multiple Waveguide Input: In this test problem, the situation is the same as that outlined for Test 4, however, instead of a single waveguide input there are two input power waveguides. For case 1), the two waveguides are located in the center of the top of the cavity at $x_1 = 7\delta x, y_1 = 5\delta y, x_2 = 7\delta x$ and $y_2 = 17\delta y$. For case 2), the two waveguides are located at staggered positions close to the sides of the top of the cavity at $x_1 = 2\delta x, y_1 = 2\delta y, x_2 = 12\delta x$ and $y_2 = 20\delta y$. The dielectric material is located at $z_0 = 21\delta z$. The aim of this test is to exhibit how the power density distribution is affected by a number of power input waveguides, and how the electromagnetics fields evolve and interact inside the lossy material for such systems. The results shown in Fig. 10 indicate that as the number of input waveguides into the cavity is increased from one to two, the shape and form of the power density changes substantially and becomes more complicated. The number of peaks present in the power density distribution increases from one to two and the locations of these peaks corresponds with, as expected, the location of the input guides. Furthermore, when the locations of these input waveguides are adjusted, there is a noticable effect on the power density distribution.

VI. Conclusion

In this paper it has been shown how the MoL technique can be used to simulate the hyperbolic Maxwell's wave equations. By comparison of the MAXMOL-H and MAXMOL-E schemes against analytical solutions for the rectangular waveguide, it is clear that the technique is accurate and that the MAXMOL-E scheme is much more convenient and computationally faster than the MAXMOL-H scheme. The reasons for the advantages of using MAXMOL-E are due to the facts that there is only one component (E_y for TE_{10} mode) which has to be computed inside the waveguide and the power density distribution generated in the dielectic material can be directly calculated from this component. However, for the MAXMOL-H scheme, there are two fields components (H_x and H_z for TE_{10} mode) which have to computed inside the waveguide, and the solution of the $\boldsymbol{H}$ field must be transformed into the $\boldsymbol{E}$ field before the power density distribution can be deduced.

The details of the MAXMOL-E method have been presented in this paper and used to analyze the electric field and power distributions in a microwave, dielectrically loaded rectangular cavity with both single- and double-input power waveguides. The algorithm has been tested against the FDTD method for the case of a simply loaded cavity where good agreement between the two methods has been noted.

In summary it was found that the MAXMOL-E method is straightforward to implement and provides a simple path for accommodating within the code such factors as multipower input and multilayered dielectric loads. The results of the two input power waveguide tests exhibited in this paper are included as a thought provoking exercise for future research that will focus on the optimization of the cavity design. This optimization seeks to achieve a uniform heating phenomenon to arise within the loaded material. The MAXMOL-E method provides all the necessary ingredients for such a study, since it can easily be utilized to investigate the effects of varying important parameters that include the dimension and shape of the cavity, the number and location of the excitation ports, and the dimension, shape, and position of the material within the cavity.

APPENDIX

Approximation for a cross direvative term at an interface between two dielectric materials

$$\begin{aligned}\frac{\partial^2 \hat{E}_y}{\partial x \partial y} &= \frac{1}{2}(DT_1 \hat{E}_{y(i-1,j-1,k)} + DT_2 \hat{E}_{y(i+1,j+1,k)} \\ &\quad - DT_3 \hat{E}_{y(i-1,j+1,k)} - DT_4 \hat{E}_{y(i+1,j-1,k)}) \\ &\quad + \frac{1}{2}(DT_5 \hat{E}_{y(i-1,j,k)} + DT_6 \hat{E}_{y(i+1,j,k)} \\ &\quad + DT_7 \hat{E}_{y(i,j-1,k)} + DT_8 \hat{E}_{y(i,j+1,k)}) \\ &\quad + \frac{1}{2} DT_9 \hat{E}_{y(i1,j,k)}\end{aligned}$$

$$DT_1 = \frac{2\varepsilon'_{(i-1,j-1,k)}}{\varepsilon'_{(i-1,j,k)} + \varepsilon'_{(i-1,j-1,k)}} + \frac{2\beta_{(i,j-1,k)}}{\beta_{(i,j-1,k)} + \beta_{(i-1,j-1,k)}}$$

$$DT_2 = \frac{2\varepsilon'_{(i+1,j+1,k)}}{\varepsilon'_{(i+1,j,k)} + \varepsilon'_{(i+1,j+1,k)}} + \frac{2\beta_{(i,j+1,k)}}{\beta_{(i,j+1,k)} + \beta_{(i+1,j+1,k)}}$$

$$DT_3 = \frac{2\varepsilon'_{(i-1,j+1,k)}}{\varepsilon'_{(i-1,j,k)} + \varepsilon'_{(i-1,j+1,k)}} + \frac{2\beta_{(i,j+1,k)}}{\beta_{(i,j+1,k)} + \beta_{(i+1,j-1,k)}}$$

$$DT_4 = \frac{2\varepsilon'_{(i+1,j-1,k)}}{\varepsilon'_{(i+1,j,k)} + \varepsilon'_{(i+1,j-1,k)}} + \frac{2\beta_{(i,j-1,k)}}{\beta_{(i,j-1,k)} + \beta_{(i+1,j-1,k)}}$$

$$DT_5 = \left(\frac{2\varepsilon'_{(i-1,j,k)}}{\varepsilon'_{(i-1,j,k)} + \varepsilon'_{(i-1,j+1,k)}} - \frac{2\varepsilon'_{(i-1,j,k)}}{\varepsilon'_{(i-1,j,k)} + \varepsilon'_{(i-1,j-1,k)}}\right) \cdot \frac{2\beta_{(i,j,k)}}{\beta_{(i,j,k)} + \beta_{(i-1,j,k)}}$$

$$DT_6 = \left(\frac{2\varepsilon'_{(i+1,j,k)}}{\varepsilon'_{(i+1,j,k)} + \varepsilon'_{(i+1,j-1,k)}} - \frac{2\varepsilon'_{(i+1,j,k)}}{\varepsilon'_{(i+1,j,k)} + \varepsilon'_{(i+1,j+1,k)}}\right) \cdot \frac{2\beta_{(i,j,k)}}{\beta_{(i,j,k)} + \beta_{(i+1,j,k)}}$$

$$DT_7 = \left(\frac{2\beta_{(i,j-1,k)}}{\beta_{(i,j-1,k)} + \beta_{(i+1,j-1,k)}} - \frac{2\beta_{(i,j-1,k)}}{\beta_{(i,j-1,k)} + \beta_{(i-1,j-1,k)}}\right) \cdot \frac{2\varepsilon'_{(i,j-1,k)}}{\varepsilon'_{(i,j,k)} + \varepsilon'_{(i,j-1,k)}}$$

$$DT_8 = \left(\frac{2\beta_{(i,j+1,k)}}{\beta_{(i,j+1,k)} + \beta_{(i-1,j+1,k)}} - \frac{2\beta_{(i,j+1,k)}}{\beta_{(i,j+1,k)} + \beta_{(i+1,j+1,k)}}\right) \cdot \frac{2\varepsilon'_{(i,j+1,k)}}{\varepsilon'_{(i,j,k)} + \varepsilon'_{(i,j+1,k)}}$$

$$\begin{aligned}DT_9 &= \left(\frac{2\varepsilon'_{(i-1,j,k)}}{\varepsilon'_{(i-1,j,k)} + \varepsilon'_{(i-1,j+1,k)}} - \frac{2\varepsilon'_{(i-1,j,k)}}{\varepsilon'_{(i-1,j,k)} + \varepsilon'_{(i-1,j-1,k)}}\right) \cdot \left(1 - \frac{2\beta_{(i,j,k)}}{\beta_{(i,j,k)} + \beta_{(i-1,j,k)}}\right) \\ &\quad + \left(\frac{2\varepsilon'_{(i+1,j,k)}}{\varepsilon'_{(i+1,j,k)} + \varepsilon'_{(i+1,j-1,k)}} - \frac{2\varepsilon'_{(i+1,j,k)}}{\varepsilon'_{(i+1,j,k)} + \varepsilon'_{(i+1,j+1,k)}}\right) \cdot \left(1 - \frac{2\beta_{(i,j,k)}}{\beta_{(i,j,k)} + \beta_{(i+1,j,k)}}\right) \\ &\quad + \left(\frac{2\beta_{(i,j-1,k)}}{\beta_{(i,j-1,k)} + \beta_{(i+1,j-1,k)}} - \frac{2\beta_{(i,j-1,k)}}{\beta_{(i,j-1,k)} + \beta_{(i-1,j-1,k)}}\right) \cdot \left(1 - \frac{2\varepsilon'_{(i,j,k)}}{\varepsilon'_{(i,j,k)} + \varepsilon'_{(i,j-1,k)}}\right) \\ &\quad + \left(\frac{2\beta_{(i,j+1,k)}}{\beta_{(i,j+1,k)} + \beta_{(i+1,j+1,k)}} - \frac{2\beta_{(i,j+1,k)}}{\beta_{(i,j+1,k)} + \beta_{(i-1,j+1,k)}}\right) \cdot \left(1 - \frac{2\varepsilon'_{(i,j,k)}}{\varepsilon'_{(i,j,k)} + \varepsilon'_{(i,j+1,k)}}\right).\end{aligned}$$

ACKNOWLEDGMENT

The computations referred to in this paper were carried out on computing equipment supplied to the School of Mathematics, Queensland University of Technology, under the Digital Equipment Agreement ERP 2057. The authors also wish to thank Dr. J. van Leersum, School of Mathematics, QUT, for the many fruitful discussions pertaining to this research.

REFERENCES

[1] I. Turner, "The modeling of combined microwave and convective drying of a wet porous material," Ph.D. dissertation, Univ. of Queensland, St. Lucia, Queensland, Australia, 1991.

[2] X. Jia, "Mathematical and experimental modeling of heat pump assisted microwave drying," Ph.D. dissertation, Department of Mechanical Engineering, Univ. of Queensland, Brisbane, Australia, 1992.

[3] F. Liu, I. Turner, and M. E. Bialkowski, "A finite-difference time-domain simulation of power density distribution in a dielectric loaded microwave cavity," *J. Microwave Power and Electromagn. Energy*, vol. 29, no. 3, pp. 138–148, 1994.

[4] F. Liu and I. Turner, "Numerical modeling techniques for simulating the microwave heating of polymer materials inside a ridge waveguide," in *Proc. Seventh Biennial Conf. Computational Techniques and Applications, CTAC95,* 1995, pp. 517–524.
[5] T. K. Ishii, "Theoretical analysis of arcing structure in microwave ovens," *J. Microwave Power*, vol. 18, no. 4, pp. 337–344, 1983.
[6] T. K. Ishii, Y. H. Yen, and R. J. Kipp, "Improvement of microwave power distribution by the use of the first order principle of geometrical optics for scientific microwave oven cavity," *J. Microwave Power*, vol. 14, no. 3, pp. 201–208, 1979.
[7] M. De Pourcq, "Field and power-density calculations in closed microwave systems by three-dimensional finite differences," *IEE Proc.*, vol. 132, pt. H6, pp. 360–368, Oct. 1985.
[8] J. Lawson and M. Berzins, *Computational Ordinary Differential Equations*, J. R. Cash and I. Gladwell, Eds. Oxford, U.K.: Clarendon, 1992, pp. 309–322.
[9] M. Berzins, P. M. Dew, and R. M. Furzeland, "Developing PDE software using the method of lines and differential algebraic integrators," *Appl. Numer. Maths.*, vol. 5, pp. 375–397, 1989.
[10] W. B. Fu and A. C. Metaxas, "Numerical prediction of three-dimensional power density distributions in a multi-mode cavity," *J. Microwave Power and Electromagn. Energy*, vol. 29, no. 2, pp. 67–75, 1994.
[11] W. B. Fu and A. C. Metaxas, "Numerical solution of Maxwell's equations in three dimensions using the method of lines with applications to microwave heating in a multi-mode cavity," *Int. J. Applied Electromagnetics and Mechanics*, 1995.
[12] D. K. Cheng, *Field and Wave Electromagnetic.* Reading, MA: Addison-Wesley, 1991.
[13] M. S. Stern, "Semivectorial polarized finite difference method for optical waveguides with arbitrary index profiles," *IEE Proc.*, vol. 135, pt. J, no. 1, pp. 56–61, Feb. 1988.
[14] A. C. Metaxas and R. J. Meredith, *Industrial Microwave Heating.* London, U.K.: Peter Peregrinus, 1983.
[15] G. Mur, "Absorbing boundary conditions for finite-difference approximation of the time-domain electromagnetic-field equations," *IEEE Trans. Electromagn. Compat.*, vol. EMC-23, no. 4, pp. 377–382, Nov. 1981.
[16] X. Jia and P. Jolly, "Simulation of microwave field and power distribution in a cavity by a three dimensional finite element method," *J. Microwave Power and Electromagn. Energy*, vol. 27, no. 1, pp. 11–22, 1992.

Huawei Zhao was born in Xian, People's Republic of China, on October 19, 1963. He received the B.Eng.(Civil) degree from the Nanjing Institute of Technology in July 1985, and the B.App.Sc.(Maths) degree from the Queensland University of Technology (QUT), Brisbane, Australia, in December 1993, where he is currently working toward the Ph.D. degree. His research work concerns the study of efficient numerical techniques for optimizing the power density distribution during the microwave heating of a lossy materials inside arbitrary shaped cavities.

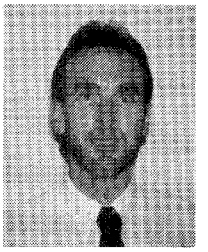

Ian Turner received the B.App.Sc. and M.Sc. degrees in mathematics from the Queensland University of Technology, Brisbane, Australia, in 1981 and 1987, respectively, and the Ph.D. degree in mechanical engineering from the University of Queensland, Brisbane, in 1991.

He is a Lecturer in the School of Mathematics at the Queensland University of Technology, and is the author or coauthor of over 50 professional papers that reflect his research interests in the design of efficient drying operations, flow in porous media, electromagnetic theory, and microwave heating, among other topics. He has established a porous media research group within the School of Mathematics at QUT which investigates heat and mass transfer phenomena that arise during complex transport problems in porous media.

Dr. Turner ia a member of the Australian Mathematical Society, and serves on the editorial board of *Drying Technology*, an international journal published by Marcel Dekker, Inc.

Fa-Wang Liu was born in Fujian Province, China, on July 10, 1949. He graduated from the Department of Mathematics of Fuzhou University, China, in 1975. He received the M.S. degree in the Department of Computer Science, Fuzhou University, in 1982, and the Doctorate degree from the School of Mathematics, Trinity College, Dublin, Ireland, in 1991.

From 1975 to 1988, he was an Associate Lecturer, a Lecturer, then Associate Professor, Department of Computer Science, Fuzhou University, China. From April 1991 to October 1991, he was a Research Fellow, Department of Mathematical Physics, University College. Since October 1991, he has been a Postdoctral Research Fellow and subsequently a Research Fellow in the School of Mathematics, Queensland University of Technology, Brisbane, Australia. His research interest is in numerical analysis and techniques for solving a wide variety of problems in applicable mathematics, including microwave heating problems, gas-solid reactions with application to the direct reduction of iron, singular perturbation problems, and semiconductor device equations.